Characterization of the CMOS camera for solid-state MASS

Authors:*A. Tokovinin, L. Peige*
Version: 1.1
Date: 2020-02-28
File: prj/atm/smass/CMOS/CMOS-study.tex

Summary: The CMOS camera ZWO ASI290 is tested. The vendor's data regarding readout noise (∼1 el) and gain are confirmed. As in most CMOS detectors, a 0.2% fraction of pixels have readout noise 3× larger than average, with a strong telegraph-like component. The maximum QE of 0.80 is found at 480 nm wavelength. A small fraction of pixels is affected by fluctuating sensitivity (spikes in the signal) and one pixel is faulty. The spatial uniformity of the response is very good, 2%.

1 Introduction

This document reports characteristics of the CMOS camera that can be used in next-generation turbulence profiler (solid-state MASS). The camera ZWO ASI290 was purchased for this purpose.[1] This product was developed primarily for astro-photography. The pixel size is 2.9 μm, format 1936×1096 pixels (size 5.6×3.2 mm), readout noise ∼1 el, maximum quantum efficiency 0.80. The detector is back-illumitated CMOS IMX290 from Sony. It is not cooled (similar cameras with cooling are available from ZWO). The camera body has a diameter of 62 mm and weights 120 g. The interface is USB 3.0. It allows a frame rate of 737.5 FPS for a ROI of 320×240 pixels.

In the solid-state MASS, the detector will read a small area at high speed (1 kHz rate) to take movies of the scintillation in a telescope pupil. The signal will be typically small, on the order of 10 photons per pixel. It is essential to have a low detector noise and to know well the noise properties. This study is conducted to clarify these aspects of the camera and to confirm its characteristics provided by the vendor.

2 Setup

The camera is connected by the USB 3.0 port to a small PC working under Ubuntu Linux. The INDI driver is installed.[2] It works as a server. An application connects to the server and works with the camera. A stand-alone software Kstars, developed primarily for astro-photography, can be used to take images.

This study used python scripts developed by L. Peige to work with the camera. The scripts are based on the INDI-py library. They allow camera control and acquisition of individual frames (full or ROI) and series of frames that can be saved as FITS files. Further details of the python software will be covered in a separate document.

The camera was installed on the detector-testing bench at the CTIO electronic lab. The bench contains an integrating sphere illuminated by a monochromator. It is equipped with a calibrated

[1] https://astronomy-imaging-camera.com/product/asi290mm
[2] https://indilib.org/

Table 1: Gain measurement on 2020-02-26

G	RON (el)	L (ADU)	g el/ADU	$g_{\rm model}$ (el/ADU)
150	1.28	68.26	0.644	0.640
250	1.07	214.5	0.204	0.203
300	0.99	386.2	0.113	0.114

power meter. The detector is installed at a fixed distance from the sphere, with a known attenuation factor relative to the power meter. Therefore, the quantum efficiency (QE) can be measured. We used an offset of 100 ADU to avoid clipping of negative values. The images are taken in the 16-bit mode. However, the camera works at 12 bit resolution. Each ADU of the camera corresponds to 16 units in the FITS images. In the following, we divide the values by 16 to recover the original 12-bit ADUs.

Analysis of the images was made by A.T. using simple IDL programs.

3 Gain and readout noise

The first tests of noise were made on February 17 by taking image cubes of 96×96 pixels with 1 ms exposure, 100 ADU offset, and a gain setting G of 200 (in the following, we use G for the gain setting to avoid confusion with the actual gain g in el/ADU). The frame rate in this mode was 810 Hz. The signal histogram (Fig. 1) has a Gaussian core with a dispersion of 3.37 ADU and asymmetric wings produced by noisy pixels. The noisy pixels have fixed location on the detector. A signal in one noisy pixel is plotted and compared to the signal in a normal pixel. Noisy pixels have a telegraphic-type signal with fixed positive or negative increments. Some asymmetry of the histogram (stronger positive wing) suggests a contribution of the dark current. However, the correlation between average signal and noise level is not obvious. As found later, the gain was 0.36 el/ADU, hence the readout noise in "normal" pixels is 1.2 el.

The first gain measurement was made on Feb. 21 using two cubes: one dark, another with a light, both with $G = 200$. Comparison between the variances and signal levels in these cubes results in $q = 0.37$ el/ADU. Gain measurements were repeated on Feb. 26 for 3 values $G = [150, 250, 300]$. At each gain, a cube of 96x100x100 size was taken without light and with a 1-ms exposure, then another cube with a 0.5 s exposure and light. The average light signal was 44 el/pixel. The cubes were processed by the IDL script `gain.pro`. The gain is evaluated by the formula

$$g = L/(\sigma_L^2 - \sigma_D^2), \tag{1}$$

where L is the light level per pixel in ADU, computed as a difference between mean signal values of two cubes, σ_L^2 and σ_D^2 are the signal variances with and without light, respectively, in ADU^2. They are evaluated as median variances in each cube and therefore are not affected by the minority of noisy pixels. The readout noise (RON) in electrons equals $g\,\sigma_D$.

The results are given in Table 1. The correctness of the gain calculation can be verified by the product gL, i.e. the number of photons per pixel, which remains constant (44.0, 43.76, 43.64) for all 3 gain settings.

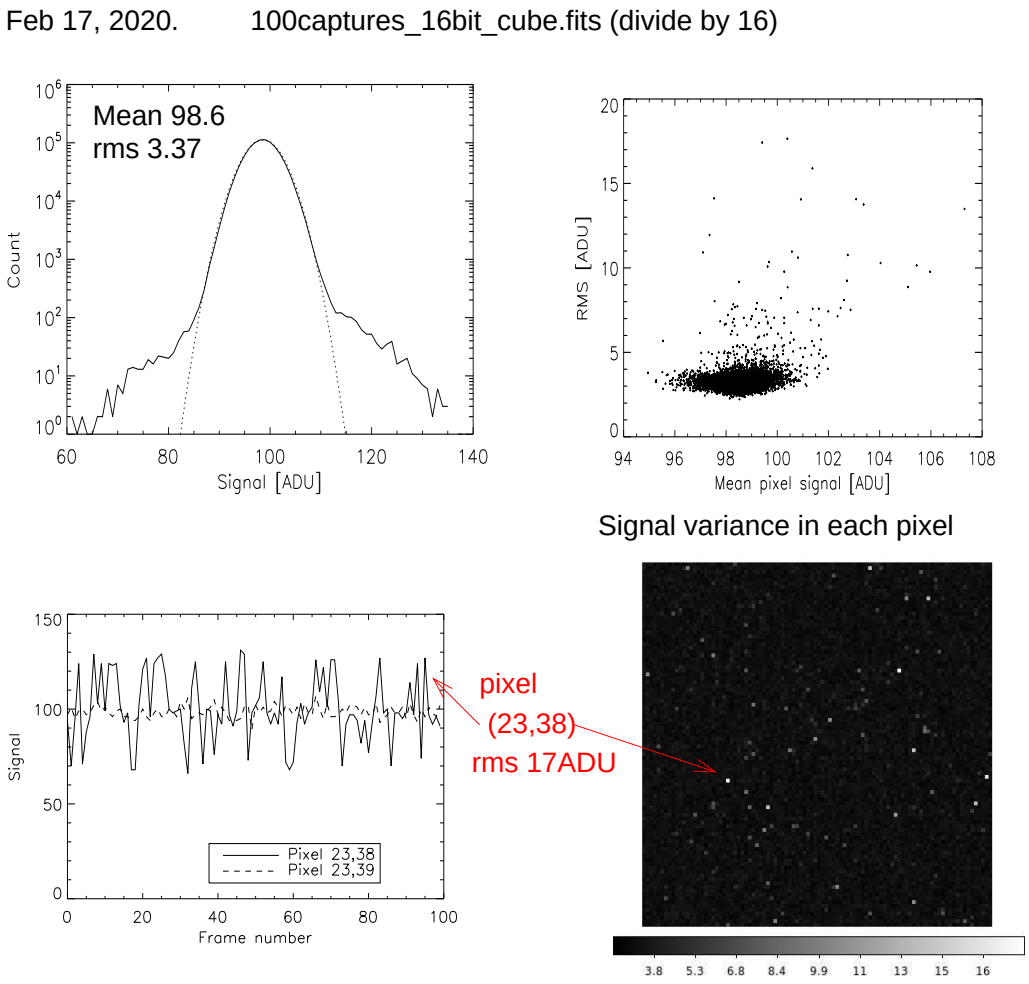

Figure 1: Noise in the dark cube of 96×96 pixels. The histogram of signal is shown in the upper left, with a dotted Gaussian curve. The image in the lower-right shows the rms scatter in each pixel of a 100×100 ROI; noisy pixels look bright and have a "telegraphic" signal.

The camera manual says that the unit of gain G is 0.1 dB. This means that 200 units of G change the gain by a factor of 10. Our data confirm this and allow to compute the gain by a simple formula

$$g_{\rm model} = 0.64\ 10^{(150-G)/200}. \qquad (2)$$

The result of this formula is given in the last column of Table 1. It matches the actual measurements within 1%. The formula indicates that $G = 200$ corresponds to $g = 0.36$, and this value is used in the following. Our measurements agree well with the plot of $g(G)$ given in the camera manual.

To characterize the signal variance in all detector pixels, two full-frame data cubes (100 images each) with and without light were taken on 2020-02-27 with $G = 200$.

The mean readout noise is 1.19 el. The noise in most pixels is close to this value, but there is a weak exponential tail of noisy pixels (Fig. 2). The fraction of pixels where the RON exceeds its mean

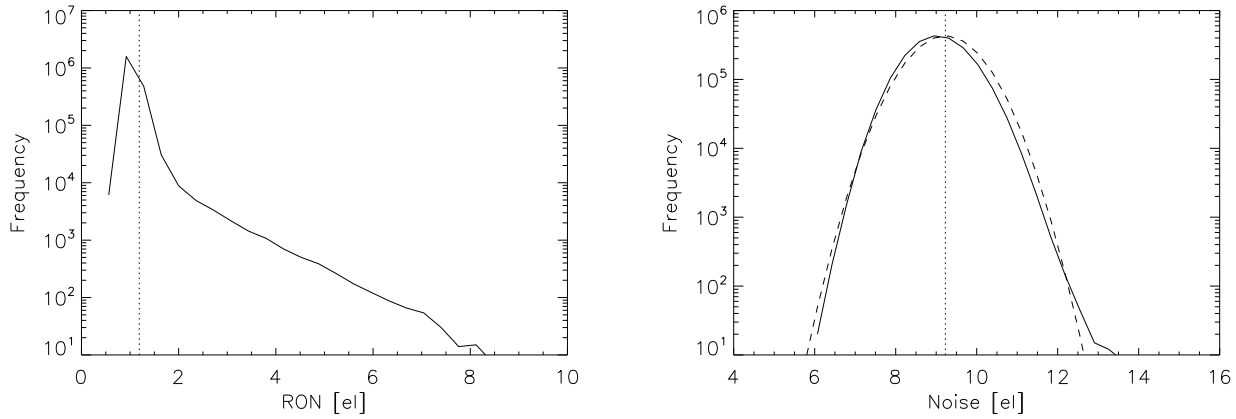

Figure 2: Distributions of the noise at $G = 200$ (note the vertical logarithmic scale) in the dark full-frame image cube (left) and with light (right). The dashed line in the right plot is a Gaussian curve.

value by a factor of 3 (above 3.6 el) is 0.00189, or about 0.2%. The distribution of RON is similar to other high-end CMOS cameras.[3]

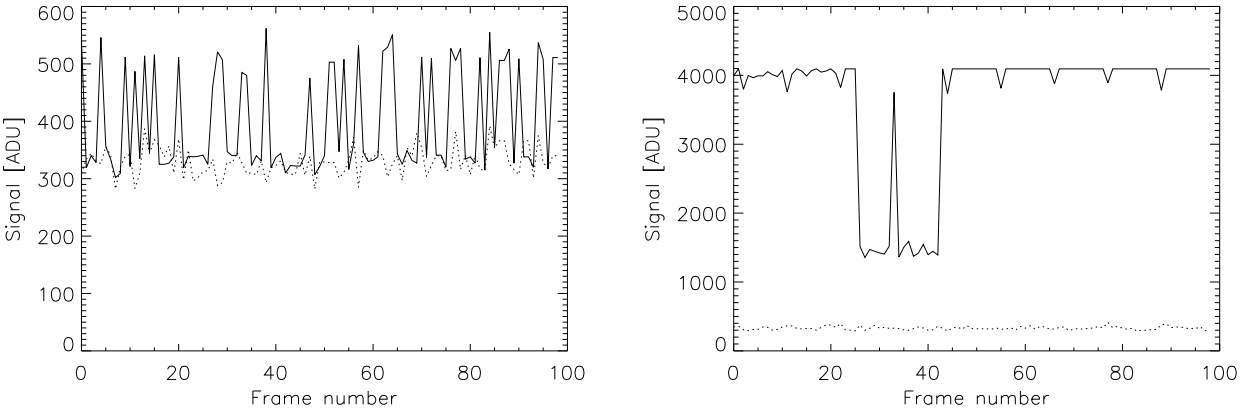

Figure 3: Signals in bad pixels with light. In both plots, the full line shows the signal in a bad pixel vs. frame number and the dotted line shows the signal in the adjacent good pixel for comparison. Left: a typical bad pixel [152, 139]. Right: the defunct pixel [1819,127].

The noise in the illuminated data cube is distributed more uniformly (Fig. 2, right). The mean value is 9.1 el, and the dispersion around this value is 0.43 el (dashed Gaussian curve). The number of pixels where the noise in the light cube exceeds its mean value by 3 times is only 19, and the number of pixels with the noise above 13 el. is 70 (3.30E-5 fraction of all pixels). Figure 3 illustrates signal

[3]See https://www.pco.de/fileadmin/user_upload/pco-product_sheets/pco.edge_42_A_data_sheet.pdf

variation in a typical bad pixel [152, 139]. It contains positive spikes. Interestingly, the signal value in the spikes is twice its normal value (after accounting for the offset of 100 ADU). One pixel [1819,127] has a huge signal variance and is apparently defectuous.

4 Quantum efficiency and uniformity

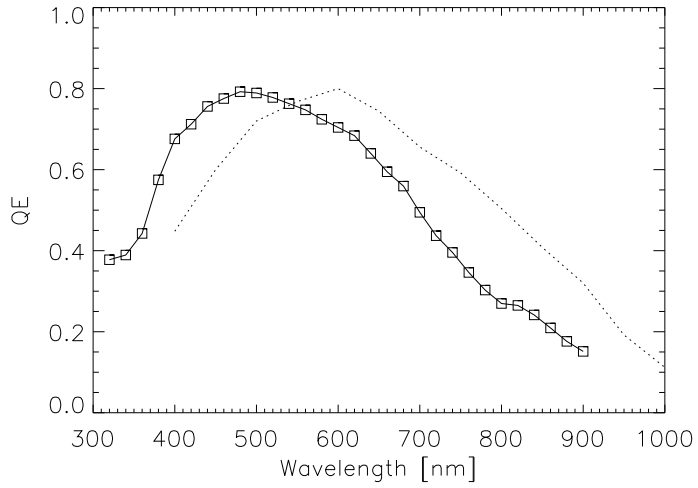

Figure 4: Quantum efficiency vs. wavelength. The dotted curve shows the vendor's plot normalized to the maximum QE of 0.8.

To measure the quantum efficiency, series of frames with a fixed exposure time of 12 s were taken. For each frame, a different monochromator wavelength λ was set (with a step of 20 nm between frames) and the power was recorded in the image header. The QE curve was calculated using the IDL code `qedata.pro`.

The number of photons received by the power meter is $N_{PM} = Wt/E_{ph}$, where W is the measured power in Watts, t is the exposure time, and $E_{ph} = hc/\lambda$ is the photon energy in Joules (3.3E-19 J for λ = 6E-7 m). Each pixel of the camera receives the number of photons $N_{pix} = FN_{PM}$, where the reduction factor F is the ratio of pixel area (2.9 μm^2) to the power-meter area (0.85 cm^2) multiplied by the additional geometric attenuation factor of 1/184 computed from the square ratio of the distances of the power meter and detector from the sphere. Knowing the pixel signal L in ADU and the gain g, we compute the quantum efficiency QE = Lg/N_{pix}.

The QE(λ) curve is plotted in Fig. 4. We confirm the vendor's data (maximum QE of 0.8), but note that the maximum is at 500 nm and not at 600 nm as specified by the vendor. Our camera has a noticeably "bluer" response compared to the vendor's data. At the shortest wavelengths, the signal is small and the QE measurement can be biased by the dark current.

The spatial detector response (flat field) is very uniform. In the averaged cube of 100 full frames taken with a 12-s exposure each and the average signal (after offset subtraction) is 2840 ADU (1025.2 el), the median rms is 32.0 el (very close to the square-root of N). After averaging the cube and

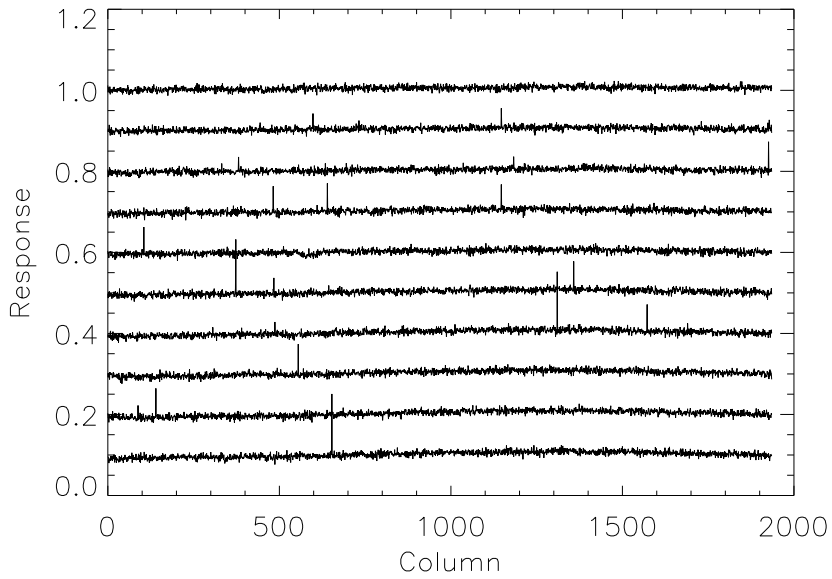

Figure 5: Normalized signal along lines 0, 100,..., 900 in the averaged full-frame cube taken with a 12-s exposure. Each line is shifted by 0.1.

normalizing it by the mean, the rms variation over the field is only 0.8%. It includes contribution from the dust shadows, so the actual uniformity can be even a little better. Figure 5 shows relative signal variation along 10 lines that sample the full detector surface. The sensitivity variation is dominated by little spikes. There are 2901 "spiky" pixels (0.00094 fraction) where the mean signal exceeds its mean level by more than 3%. The median noise level in these pixels is same as in the normal ones, which means that the spikes correspond to real gain variation and/or to a strong dark current. In this 12-s cube, the actual bad pixels (see Fig. 3) are saturated (maximum signal 4096 ADU at 12 bit).

5 Further work

The CMOS camera studied here has a very low noise and a good QE. Its dark current has not yet been measured, but for the intended application in solid-state MASS (very short exposures) it is not relevant.

To complete the camera evaluation, we need to take a long (e.g. 1-s) series of consecutive short-exposure frames (with ROI) with a regularly variable light source to investigate the continuity of the data stream (check for missing frames).